

## Intermolecular Interactions in Bithiophene as a Model for Polythiophene

Lambert van Eijck,<sup>\*,†</sup> Mark R. Johnson,<sup>‡</sup> and Gordon J. Kearley<sup>†</sup>

*Interfaculty Reactor Institute, Delft University of Technology, Mekelweg 15, 2629 JB Delft, The Netherlands, and Institut Laue-Langevin (ILL), BP 156, 38042 Grenoble, Cedex 9, France*

*Received: May 8, 2003; In Final Form: August 20, 2003*

Intra- and intermolecular interactions in bithiophene are investigated via the measured and calculated vibrational density of states for the polycrystalline material. There is strong intermolecular interaction that hardens vibrational coordinates with respect to the isolated molecule, especially the inter-ring torsion. The torsional barrier of the isolated molecule is understood in terms of delocalization energy, nonbonded intramolecular interaction, but in the solid the barrier is dominated by intermolecular interaction. A topological analysis of the calculated electron density provides a local interpretation of intermolecular bonds that give rise to the intermolecular interactions. The results for this simple conjugated system are important for the extension to polythiophene and other conducting polymers.

### Introduction

Bithiophene is of interest as a model system for conjugated polymers, in particular polythiophene.<sup>1</sup> The interest here arises from the long-range delocalization of the  $\pi$ -systems on neighboring rings that gives rise to a small HOMO/LUMO gap that can be tuned for conducting/semiconducting purposes. To understand these properties in practical systems, we need to investigate how the dynamics of a model system affect the instantaneous electronic structure of the conjugated systems. It is convenient to begin with a vibrational analysis of crystalline bithiophene, this being a comparatively well-defined system. Further, it is small enough to allow calculation of both inter- and intramolecular interactions from first principles and we can then compare the predictions with existing experimental data for structure and dynamics.

First-principles calculations frequently use the isolated molecule approximation, and this can have serious consequences when the predictions are compared with experimental data for dynamics in the solid state. In vibrational analyses these discrepancies are often scaled out, but then it is impossible to assess the quality of the quantum-chemistry calculation for intermolecular interactions. In the present work we use the available inelastic neutron scattering (INS) spectra<sup>2</sup> as our experimental data. In this spectroscopy we are able to compare observed and calculated spectra directly because the intensities are simply related to atomic displacements and peak shapes can also be calculated. Further, INS measures the vibrational density of states, not simply the  $k = 0$  (or  $\Gamma$ -point) spectrum, so that we are sensitive to the effects of dispersion via peak shape and spectral profile. Both local solid-state effects and dispersion reflect the intermolecular interactions and it is useful to see how well quantum-chemistry calculations are able to reproduce these. Assuming this to be adequate, the same methods (or parameters derived from these) can be used for larger polymeric systems.

### Density Functional Theory Vibrational Calculations

A number of codes are now available for performing periodic density functional theory (DFT) calculations, and these were recently assessed in the calculation of INS spectra of durene.<sup>3</sup> In the present work we have used VASP<sup>4</sup> and DMol3,<sup>5</sup> the former using plane-wave basis functions to develop the electron density, whereas the latter uses localized, numerical atomic orbitals. For both codes, more or less standard settings, with only a few modifications, were used. For most of the DMol3 calculations, a DND double numerical basis set with polarization functions for carbon was used. The radial extent of the integration mesh was 10 au and the angular grid was adjusted to give a numerical precision of 0.0001. All calculations with VASP were performed using the generalized gradient approximation of Perdew and Wang (PW91) for the exchange-correlation energy and Vanderbilt-type ultrasoft pseudopotentials. The recommended energy cutoff (396 eV) for the plane wave basis set and a  $k$ -point spacing of  $0.1 \text{ \AA}^{-1}$  were used.

The vibrational spectra were calculated in the harmonic approximation using the direct method to obtain the forces. Starting from the equilibrium geometry, atoms in the asymmetric unit are displaced along the three Cartesian directions. For each perturbed structure, an energy calculation gives the Hellmann–Feynman forces on all the atoms from which the force constants are obtained by dividing by the displacement. The force-constant matrix  $\mathbf{F}$  is then transformed to mass-dependent coordinates by the  $\mathbf{G}$  matrix giving the dynamical matrix. Diagonalization of the dynamical matrix gives the vibrational eigenvalues and eigenvectors.

The program CLIMAX<sup>6</sup> was used to calculate the neutron spectral profile, corresponding to the measured spectrum, from the  $\Gamma$ -point, normal modes. The normal vibrational coordinates are mass-weighted, the scattering cross-sections of the different atoms are taken into account, overtone and combination frequencies are included, and the recoil of molecules is incorporated by convoluting the calculated peaks with the low-energy phonon spectrum (either measured or calculated).

The full phonon spectrum was calculated using the program PHONON.<sup>7</sup> Whereas a  $\Gamma$ -point-only calculation is exact for a

\* Corresponding author. E-mail: [eijck@iri.tudelft.nl](mailto:eijck@iri.tudelft.nl).

<sup>†</sup> Delft University of Technology.

<sup>‡</sup> Institut Laue-Langevin.

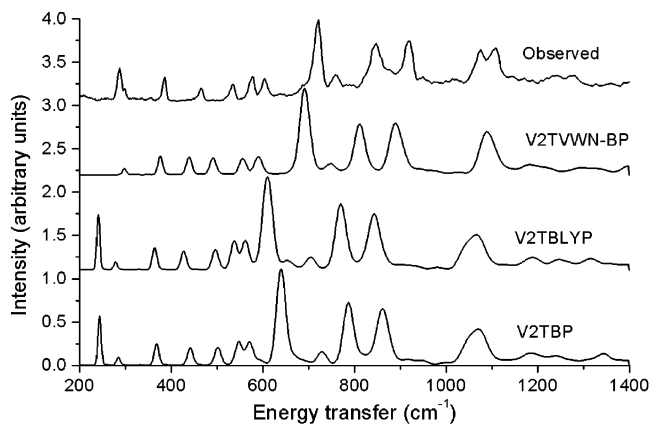


**Figure 1.** Comparison of observed INS spectrum of solid bithiophene at 20 K with calculated spectra using different functionals (DMol3). No scaling has been applied.

single unit cell, accurate dispersion relations require a supercell to be used that spans the range of typical interactions. When an atom at the center of the supercell is displaced, the forces on the atoms at the cell boundary should be zero. For bithiophene, a (1,1,2) supercell of dimensions  $a = 8.93 \text{ \AA}$ ,  $b = 7.73 \text{ \AA}$ ,  $c = 11.46 \text{ \AA}$ ,  $\gamma = 73.8^\circ$  (Kovalev setting) was used, with a factor of 1000 between the strongest and weakest force constants. The dynamical matrix is constructed for the supercell from a series of single point energy calculations on perturbed structures, as described above. To generate the density of states, the generalized dynamical matrix is diagonalized at a large number (1000) of randomly chosen points in reciprocal space. The INS spectrum is calculated as above, with up to 5 multiple phonon contributions of all inter- and intramolecular modes, included to account for overtones, combinations and molecule recoil, for the particular  $Q$ -trajectory of the instrument and convoluting with the instrument resolution function.

## Results and Discussion

**Isolated Molecule Vibrations.** INS spectra of bithiophene are illustrated in Figure 1 along with calculated INS spectra from various DFT options using an isolated molecule model. Agreement between observed and calculated data in the 250–650  $\text{cm}^{-1}$  region is quite good, and in a previous paper<sup>8</sup> we showed that this spectral region is sensitive to the orientation angle between the thiophene rings. However, above 650  $\text{cm}^{-1}$  the agreement between observed and calculated INS spectra is less satisfactory, and below 250  $\text{cm}^{-1}$  there is little agreement. In this low-frequency region intermolecular interactions are expected to play an important role, and it is thus not surprising that agreement is poor. Nevertheless, it is surprising that the agreement in the 250–650  $\text{cm}^{-1}$  region is better than in the region above 650  $\text{cm}^{-1}$ , because here the vibrations are quite “hard”. In the absence of strong hydrogen bonds we do not anticipate much effect from intermolecular interactions in this region.

Previous authors<sup>2</sup> have overcome these discrepancies by using different scale factors in different spectral regions when an isolated molecule approximation is used. However, this approach effectively throws the intermolecular information away. Unfortunately, error-cancellation in DFT methods is still somewhat unpredictable, particularly for weaker long-range interactions, and it is important to test the calculations against experimental data. It is widely believed that deviations from coplanarity between the  $\pi$ -systems of conjugated polymers are an important factor in the conductivity of the polymer chains.<sup>9</sup> We will show

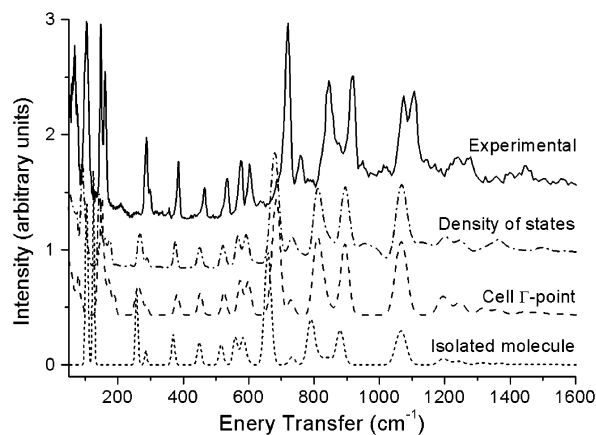


**Figure 2.** Comparison of experimental INS spectrum of solid bithiophene (20 K) with spectra calculated using DFT (VASP) with different treatment of solid-state effects.

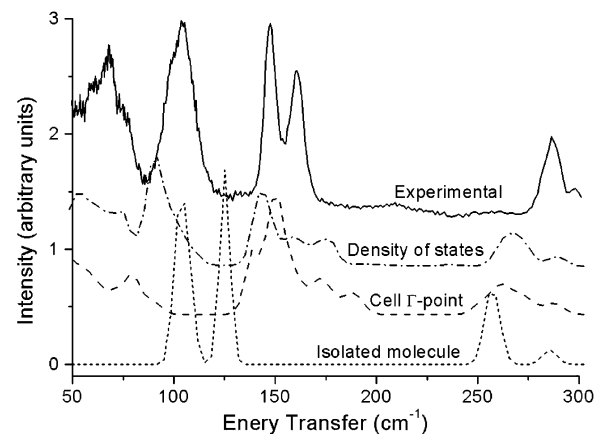


**Figure 3.** Low-energy region of the INS spectrum of solid bithiophene (20 K) compared with spectra from DFT calculations (VASP) with different treatment for solid-state effects.

the rotational potential of the intermonomer angle is dramatically increased in the solid state.

**Periodic Model Vibrations.** There are now a number of standard quantum-chemistry packages that allow DFT methods to be applied to periodic systems. We found that VASP and DMol3 gave very similar results, so in the vibrational part of this work we will refer only to results from VASP. Energy minimization of the published crystal structure<sup>10</sup> resulted in only small atomic displacements, the unit-cell parameters being constrained to the experimental values. This result is encouraging because it shows that the calculated potential-energy minima for the atoms correspond well with the experimental atomic positions. The experimental INS spectrum is compared with the calculated spectra for an isolated molecule and the energy-minimized periodic model in Figure 2. It is clear from the figure that the periodic model gives a marked improvement in the agreement in the 50–250  $\text{cm}^{-1}$  region, an expansion of this region being illustrated in Figure 3. We conclude that the calculation seems to take reasonable account of the intermolecular interactions. Perhaps surprisingly, the periodic model also does better in the higher frequency region above 650  $\text{cm}^{-1}$ , there being a significant upward shift of most bands toward the experimental features, and the overall agreement of intensities is also improved. Clearly, there are solid-state effects in this spectral region and we will look into these later in the paper.

**Dispersion of Vibrations.** Intermolecular interactions over longer ranges lead to dispersion, which because of the incoherent

**TABLE 1: Observed and Calculated Frequencies for the Full Solid-State Calculations<sup>a</sup>**

approximate assignment	obs (cm <sup>-1</sup> )	calc (cm <sup>-1</sup> )
Ag ring deformation	287	269
Ag ring deformation	385	376
Ag ring deformation	758	733
Ag ring deformation	919	900
Ag CH bend	1075	1071
Ag CH bend	1075	1071
Bg ring puckering	534	523
Bg ring puckering	602	593
Bg outer CH bend	721	680
Bg CH bend	847	813
Bg CH bend	919	897
Au ring puckering	465	453
Au ring puckering	577	566
Au outer CH bend	721	680
Au CH bend	847	813
Au CH bend	919	897
Bu ring deformation	758	733
Bu ring deformation	919	897
Bu outer CH bend	1075	1071
Bu CH bend	1107	1071

<sup>a</sup> These wavenumbers correspond to maxima in the density of states and are not directly comparable with the long-wavelength limit values measured by IR and Raman spectroscopies. For simplicity, however, the symmetry species are for the point group.

neutron scattering process leads to the measurement of a density of states in the experimental INS spectrum. Because there is still some residual disagreement between the experimental INS spectrum and that calculated from the periodic model, it is interesting to inquire whether taking account of dispersion can reduce this disagreement. The spectrum was collected using the TFXA instrument at the ISIS facility in the U.K., which works in a so-called “inverted geometry” or fixed final-energy mode. Because the final neutron-energy is small compared with the energy transfer, the momentum transfer,  $Q$ , is approximately proportional to square root of the energy transfer,  $E$ , with a proportionality constant of 0.2438 for  $Q$  in Å<sup>-1</sup> and  $E$  in cm<sup>-1</sup>. Each spectral point is then proportional to the density of states up to the corresponding value of  $Q$ , and if the dispersion is calculated, it is straightforward to produce the predicted TFXA spectrum.

The results of the “full-phonon” calculation are also shown in Figures 2 and 3 where they are compared with both the experimental INS spectrum and the calculated  $\Gamma$ -point ( $k = 0$ ) calculation. Wavenumber data are collected in Table 1. Above 250 cm<sup>-1</sup> the improvement is very slight, the modes being almost undispersed. The region below 250 cm<sup>-1</sup> is shown on an expanded scale in Figure 3. Though an improvement in this region is achieved by using a periodic model rather than an isolated molecule, there is further improvement when dispersion is also included. This is a further indication that the DFT method used in this work reproduces the vibrational effects of intermolecular interactions on those modes that are highly populated at around room temperature, and which are particularly relevant to conducting polymers.

**Rotational Potentials.** Having established that DFT at this level provides reasonable intermolecular interactions, we can now investigate the role of these interactions in more detail. The difference between the measured and calculated conductivities of isolated polythiophene chains is thought to be due to dynamic disorder and local chain defects. It seems reasonable to expect that increasing disorder of the rotational angle between monomers will play an important role in reducing the conductivity, and in real solid-state systems intermolecular interactions

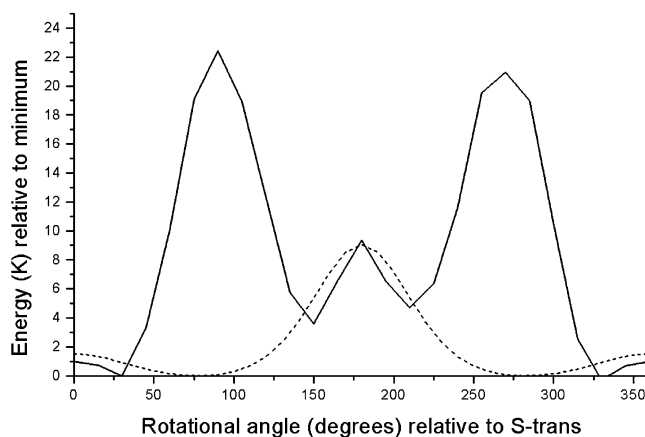


**Figure 4.** Comparison of the total rotational potential for an isolated bithiophene molecule calculated by DFT (DMol3) (solid line), with the van der Waals contribution to this potential calculated with a force-field method (compass) (dashed line). The magnitude of the van der Waals contribution has been rescaled to the submaximum of the total potential.

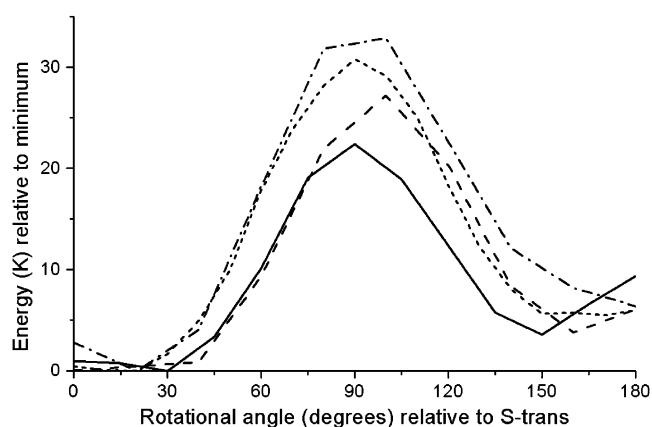


**Figure 5.** Barrier to rotation of terminal thiophene units in: bithiophene (solid line), terthiophene (dashed line), quaterthiophene (dot-dash line), and sexithiophene (short-dash line). These calculations were made using DFT (DMol3) for the isolated molecules.

may make an important contribution to local rotational barriers. Our calculation of the rotational potential using DMol3 for an isolated molecule agrees with that previously published<sup>9</sup> and has the form illustrated in Figure 4. Although the molecule adopts a flat orientation in the crystal, in the isolated molecule the monomers are twisted by 27° with respect to each other in the minimum-energy conformation. This is a result of weak interaction of the hydrogen atoms nearest to the inter-ring bond, as is confirmed by the reduction in the inter-monomer dihedral angle when the C–C–H angles are constrained to reduce the interaction of these hydrogen atoms. In Figure 4 we also include the rotational potential of bithiophene using only the “non-bonded” terms of an ab initio based force field (compass<sup>11</sup>). Here it is clear that the delocalization energy has a minimum at 0° whereas the “nonbonded” energy has a minimum at 80°, the sum of the two functions having a minimum at 27°.

We have also calculated the rotational potentials of ter-, quater- and sexithiophene, and these are illustrated in Figure 5. As the conjugated system becomes longer, the delocalization energy increases, whereas the “nonbonded” interactions are unchanged. This results in an increase of the rotational barrier with the minima shifting more toward 0° and 180° (subminimum for cis configuration).

For crystalline bithiophene we have used a cluster model of 7 molecules to estimate the intermonomer rotational potential

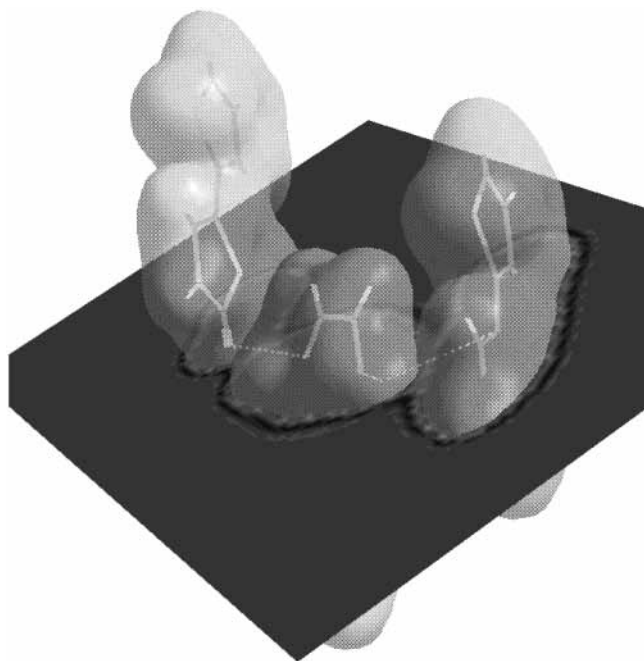


**Figure 6.** Electron density isosurface for a bithiophene cluster with the orientations as found in the crystal structure. The dotted lines show calculated bond paths, with the slice illustrating the plane in which the bond-paths lie.

in the solid state. This calculation could also have been made for a periodic model using a considerably larger cell, but this would be unnecessarily time-consuming, particularly considering that nearest-neighbor interactions are the most important. In this case we did not allow the structure of the cluster to relax during the rotation, which clearly leads to a falsely high total barrier. Nevertheless, the torsional force-constant taken from the curvature of the potential close to the minimum is fairly insensitive to this approximation and we find that the torsional force constant is 5 times greater in the solid state than for the isolated molecule. Even in a poorly crystalline polymer the intermolecular interactions are similar and would lead to a considerable stiffening of the rotational freedom of the chain.

**Directional Interactions in the Solid State.** The intermolecular interactions are manifest in the shifts of the vibrational frequencies in going from the isolated molecule to the periodic system. Because there are significant shifts even for modes at almost  $1000\text{ cm}^{-1}$ , these interactions are quite strong, although they do not lead to dispersion in this spectral region. Rather than mapping out pair potentials to determine where these stronger interactions lie, we use a topological analysis of the calculated total electron density ( $\bar{\rho}$ ) map to determine bond paths within the formalism proposed by Bader.<sup>12</sup> We start by locating the critical points in the electron density, that is, where the gradient of the electron density  $\nabla\bar{\rho}(\bar{r})$  vanishes. In addition to the maxima associated with atom positions, there are also saddlepoints where the curvature is positive in one direction and negative in the two others. Saddlepoints are located somewhere between the nuclei and are usually termed “bond critical points”. The next step is to identify gradient paths, i.e., curves, such that the gradient vector  $\nabla\bar{\rho}(\bar{r})$  is tangent to it in every point. Paths that originate at a bond critical point and lead to atoms can be thought of as corresponding to bonds. We perform this topological analysis on the electron density with the program FAST,<sup>13</sup> the results for the bond critical points and the path for the model being shown in Figure 6.

We would anticipate that those vibrations that change most on going from the calculations for isolated molecule to the

$\Gamma$ -point calculation would involve the greatest change in the lengths of the intermolecular bonds calculated above. This expectation is fulfilled, the greatest changes in intermolecular bond-lengths being for modes observed at  $721$ ,  $847$ , and  $1071\text{ cm}^{-1}$ , these also being the modes for which the agreement between observed and calculated spectra is least satisfactory. The greatest intermolecular bond distortion is for the mode at  $721\text{ cm}^{-1}$ , for which the agreement between observation and calculation is particularly troublesome. It would seem that the bond paths calculated from the electron density do indeed illustrate the most important intermolecular interactions and it may be possible to develop a force field using these for future molecular dynamics simulations of related systems.

## Conclusions

An understanding of conduction in polymers requires reliable electronic structure calculations and a reliable description of static and dynamic disorder. In the present paper we have shown that at the appropriate level, DFT is capable of reproducing the structure and dynamics of bithiophene, which is the dimeric analogue of polythiophene. We can therefore conclude that this method is suitable for structure and dynamics of larger systems and further that the calculated electronic structures are reliable.

Comparisons of DFT calculations with IR and Raman spectra have the disadvantage that peak intensities vary strongly and are difficult to calculate. Comparison of frequency data alone can be risky in systems as large as bithiophene. Further, these spectroscopies measure at the long-wavelength limit and provide no information on important interactions that lead to dispersion. In the present work we have gone much further than an isolated molecule calculation, and though the agreement between observation and calculation improved considerably, the residual differences in the region above  $750\text{ cm}^{-1}$  seem to be at the limit of the technique. For the DFT method as used in the present work, dispersive interactions are missing, and in a molecular crystal such as bithiophene this could easily be the main source of the residual error. We could of course scale these differences out, because the calculated spectral profile is rather good but that is not the aim of the present work.

The intramolecular rotational potential is very weak but this is increased considerably by the intermolecular interactions that also affect some relatively high-frequency vibrations. A convenient method of visualizing these interactions, and understanding how they affect the dynamics, is by finding bond paths in the electron-density maps of a cluster model. These could be useful in understanding local disorder that is important in the conductivity of the polymeric system.

**Acknowledgment.** We gratefully acknowledge F. Zerbetto for allowing us to use the INS spectrum, and L. D. A. Siebbeles for useful discussions. This work was partly financed by The Netherlands Foundation for Fundamental Research of Matter (FOM).

## References and Notes

- (1) Yu, Z. G.; Smith, D. L.; Saxena, A.; Martin, R. L.; Bishop, A. R. *Phys. Rev. Lett.* **2000**, *84*, 721.
- (2) Esposti, A. D.; Zerbetto, F. *J. Phys. Chem. A* **1997**, *101*, 7283.
- (3) Plazanet, M.; Johnson, M. R.; Gale, J. D.; Yilderim, T.; Kearley, G. J.; Fernandez-Diaz, M. T.; Sanchez-Portal, D.; Artacho, E.; Soler, J. M.; Ordejon, P.; Garcia, A.; Trompsdorff, H. P. *Chem. Phys.* **2000**, *261*, 189.
- (4) Kresse, G.; Furthmuller, J. Software VASP, Vienna 1999; *Phys. Rev. B* **1996**, *54*, 11, 169; *Comput. Mater. Sci.* **1996**, *6*, 15.
- (5) Delley, B. *J. Chem. Phys.* **1995**, *92*, 508–517.
- (6) Kearley, G. J. *Nucl. Instrum. Methods Phys. Res. A* **1995**, *53*, 354.

- (7) Parlinski, K. *Am. Inst. Phys. Conf. Proc.* **1999**, 479, 121.
- (8) van Eijck, L.; Siebbeles, L. D. A.; Grozema, F. C.; de Schepper, I. M.; Kearley, G. J. *Appl. Phys A* **2002**, 74, 496.
- (9) Grozema, F. C.; van Duijnen, P. T.; Berlin, Y. A.; Ratner, M. A.; Siebbeles, L. D. A. *J. Phys. Chem. B* **2002**, **106**, 7791.
- (10) Pelletier, M.; Brisse, F. *Acta Crystallogr. C* **1994**, 50, 1942.
- (11) Sun, H. *J. Phys. Chem. B* **1998**, 102, 7338.
- (12) Bader, R. F. W. *Atoms in Molecules. A Quantum Theory*; Clarendon Press: Oxford, 1990.
- (13) <http://www.nas.nasa.gov/Software/FAST/>.